

# Unified Shrinkage Model for Concrete from Autogenous Shrinkage Test on Paste with and without Ground-Granulated Blast-Furnace Slag

by Ya Wei, Will Hansen, Joseph J. Biernacki, and Erik Schlangen

*Autogenous shrinkage development was studied as a function of time for cement paste and concrete hydrating under sealed conditions at room temperature. Effects of water-cementitious material ratio (w/cm) (0.35, 0.40, and 0.45), ground-granulated blast-furnace slag (GGBFS) content as a percentage of total cementitious material (0, 30, and 50%) by mass, and aggregate content (40%) by volume on shrinkage development was obtained. Shrinkage measurements started after 10 hours and lasted up to 90 days. Self-desiccation (that is, reduction in pore humidity) was predicted using the HYMOSTRUC model. The effects of w/cm on shrinkage development can be normalized from shrinkage versus pore humidity curves for portland-cement paste. The aggregate effect on autogenous shrinkage was found to follow a Pickett model developed for drying shrinkage. These results suggest that a unified shrinkage model, which combines autogenous and drying shrinkage, exists. The framework for such a model is presented, which incorporates relative humidity (RH), aggregate content, and restraint factor as major variables. GGBFS initially reduces shrinkage as it behaves as a filler, thus increasing the effective w/cm. While the long-term shrinkage is increased, the major factor is most likely a reduction in pore humidity associated with pozzolanic reactions. Due to a higher internal RH in a 0.45 w/cm system, the pozzolanic effect on autogenous shrinkage is more pronounced at later ages.*

**Keywords:** aggregate; autogenous shrinkage; ground-granulated blast-furnace slag; hydration products; self-desiccation; shrinkage modeling.

## INTRODUCTION

Cement hydration without access to external water (that is, sealed curing) consumes pore water, resulting in self-desiccation (that is, reduction in pore humidity) of the paste.<sup>1</sup> A reduction in pore humidity activates internal stress-producing mechanisms (capillary, surface tension) and shrinkage occurs. The extent of self-desiccation and reduction in internal relative humidity (RH) depends on the initial water-cementitious material ratio (w/cm) and degree of hydration of the cement.<sup>2-6</sup> Shrinkage development due to self-desiccation is called autogenous shrinkage and is characterized by a uniform volume reduction, whereas drying shrinkage is the result of external drying. Thus, autogenous shrinkage at any time is a material property (that is, no moisture gradient), whereas drying shrinkage development is size-dependent and nonuniform.

Autogenous shrinkage is intensified in high-performance concrete (relative to conventional concrete) due to its generally higher cement content, reduced w/cm, and pozzolanic mineral admixtures.<sup>7,8</sup> Prior results indicate that ground-granulated blast-furnace slag (GGBFS) blended cement pastes produce somewhat greater autogenous shrinkage than neat portland-cement pastes.<sup>9-11</sup> The reasons were generally attributed to the higher chemical shrinkage,

the finer pore structure, removal of calcium hydroxide as a shrinkage restraint, and a reduction in pore humidity associated with pozzolanic reactions.

## RESEARCH SIGNIFICANCE

The objectives of this study are: 1) to determine if autogenous shrinkage of concrete can be predicted from paste shrinkage and aggregate content and restraining effect. This can provide a link to drying shrinkage prediction, which is hampered by the size effect and extended drying times (1 year or more) needed to extrapolate equilibrium shrinkage at a given RH; and 2) to determine the causes for the observed increase in later-age (longer than 7 days) autogenous shrinkage reported in several studies<sup>7,10-12</sup> for portland-cement pastes/concretes containing slag or silica fume. The ultimate goal is to achieve a more environmentally friendly and sustainable concrete, wherein high cement replacement levels with a supplementary cementitious material (SCM), such as GGBFS, is used to its fullest benefit in concrete applications (that is, lower early-age shrinkage and cracking risk, neutralized long-term shrinkage as compared to concrete without an SCM, and substantial improvements in frost and alkali-silica reaction [ASR] resistance).

## EXPERIMENTAL INVESTIGATION

### Materials

Type I ordinary portland cement (OPC) was used for preparing cement paste. As an SCM, GGBFS was used for the purpose of evaluating the effect of pozzolanic reaction on autogenous shrinkage and on the hydration products. Replacement levels of GGBFS of 30 and 50% of the total cementitious material by mass were used. Grade 120 GGBFS was used in this work. The physical properties and chemical composition of each material is listed in Table 1.

### Mixture proportioning

The mixture proportioning of cement paste and concrete is presented in Tables 2 and 3, respectively.

Cement paste was mixed in a pan mixer. For blended systems, the GGBFS was first dry-mixed with portland cement for several minutes to achieve a uniform distribution of the solid ingredients. Water was then added to the dry ingredients and mixed for another 3 minutes. The fresh paste

*ACI Materials Journal*, V. 108, No. 1, January-February 2011.

MS No. M-2008-364.R1 received March 10, 2010, and reviewed under Institute publication policies. Copyright © 2011, American Concrete Institute. All rights reserved, including the making of copies unless permission is obtained from the copyright proprietors. Pertinent discussion including authors' closure, if any, will be published in the November-December 2011 *ACI Materials Journal* if the discussion is received by August 1, 2011.

ACI member **Ya Wei** is a Lecturer in the Department of Civil Engineering at Tsinghua University, Beijing, People's Republic of China. She received her PhD from the University of Michigan, Ann Arbor, MI. Her research interests include development and characterization of cementitious composites, pavements design, and performance analysis.

**Will Hansen**, FACI, is a Professor in the Department of Civil and Environmental Engineering at the University of Michigan. He is the Chair of ACI Committee 231, Properties of Concrete at Early Ages, and a member of ACI Committees 209, Creep and Shrinkage in Concrete, and 224, Cracking. His research interests include blended cements, testing, curling and warping, and pavement performance.

**Joseph J. Biernacki**, FACI, is a Professor in the Department of Chemical Engineering at Tennessee Technological University, Cookeville, TN. His research interests include multi-scale characterization and modeling of cementitious materials.

ACI member **Erik Schlangen** is an Associate Professor in the Department of Design and Construction at Delft University of Technology, Delft, the Netherlands. His research interests include fracture mechanics of cement-based material, early-age material properties and cracking of concrete, and testing and modeling of damage mechanisms.

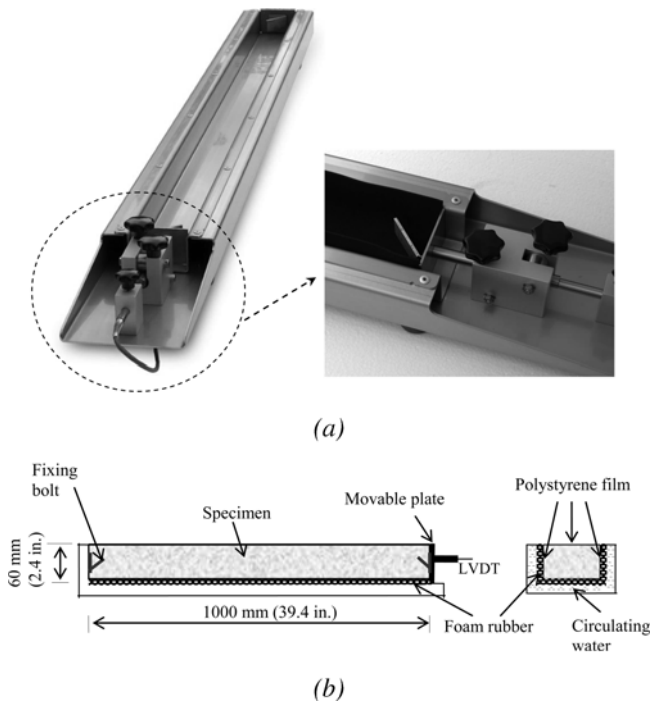


Fig. 1—One-dimensional measurement of autogenous shrinkage of cementitious system: (a) photos<sup>13</sup>; and (b) schematic illustration of apparatus.

was consistent and uniform with no visible agglomerates in the mixture. For the autogenous shrinkage measurements, to avoid bleeding, the cement paste was allowed to hydrate in the pan mixer overlaid with plastic foil for approximately 3 to 4 hours for the higher  $w/cm$  pastes, prior to casting. Mixing commenced every half hour to maintain workability. The autogenous shrinkage of concrete with 40% aggregate content by total mixture volume was measured at three  $w/cm$ : 0.35, 0.4, and 0.45. The coarse aggregate was crushed limestone with a maximum size of 12.5 mm (0.5 in.). The fine aggregate was natural sand with a fineness modulus of 2.56. Some adjustment to the amount of high-range water-reducing admixture was made to achieve consistent rheological properties for better workability. Air-entraining admixture (AEA) was used as needed to obtain 5 to 7% air in the concrete mixtures.

**Table 1—Physical properties and chemical compositions of cementitious materials**

	OPC	GGBFS
Blaine fineness, $cm^2/g$	4290	6020
SiO <sub>2</sub> , %	20.4	37.49
Al <sub>2</sub> O <sub>3</sub> , %	5.04	7.77
Fe <sub>2</sub> O <sub>3</sub> , %	2.51	0.43
CaO, %	62.39	37.99
MgO, %	3.43	10.69
SO <sub>3</sub> , %	2.75	3.21
Na <sub>2</sub> O, %	0.25	0.28
K <sub>2</sub> O, %	0.67	0.46
Cl	0.03	—
Total as oxides	97.47	—
C <sub>3</sub> S	53.66	—
C <sub>2</sub> S	18.01	—
C <sub>3</sub> A	9.11	—
C <sub>4</sub> AF	7.64	—

**Table 2—Mixture proportioning of cement paste**

Material	$w/cm = 0.35$			$w/cm = 0.45$		
	OPC	30% GGBFS	50% GGBFS	OPC	30% GGBFS	50% GGBFS
Cement, lb/yd <sup>3</sup> (kg/m <sup>3</sup> )	2528 (1500)	1770 (1050)	1264 (750)	2196 (1303)	1537 (912)	1098 (651)
GGBFS, lb/yd <sup>3</sup> (kg/m <sup>3</sup> )	—	758 (450)	1264 (750)	—	659 (391)	1098 (651)
Water, lb/yd <sup>3</sup> (kg/m <sup>3</sup> )	885 (525)	885 (525)	885 (525)	988 (586)	989 (587)	989 (587)

**Table 3—Mixture proportioning of concrete with aggregate content of 40%**

Material	$w/cm = 0.35$	$w/cm = 0.4$	$w/cm = 0.45$
Cement, lb/yd <sup>3</sup> (kg/m <sup>3</sup> )	1286 (763)	1192 (707)	1112 (660)
Water, lb/yd <sup>3</sup> (kg/m <sup>3</sup> )	450 (267)	477 (283)	501 (297)
Limestone, lb/yd <sup>3</sup> (kg/m <sup>3</sup> )	452 (268)	452 (268)	452 (268)
Sand, lb/yd <sup>3</sup> (kg/m <sup>3</sup> )	1286 (763)	1286 (763)	1286 (763)
Air-entraining admixture, lb/yd <sup>3</sup> (kg/m <sup>3</sup> )	2.5 (1.5)	2.3 (1.38)	2.2 (1.32)
Water-reducing admixture, lb/yd <sup>3</sup> (kg/m <sup>3</sup> )	5.2 (3.1)	—	—

### One-dimensional autogenous shrinkage measurement

One-dimensional autogenous shrinkage was measured on sealed specimens using a double-walled, water-cooled, stainless steel apparatus,<sup>13</sup> as shown in Fig. 1. The specimen cross section was 60 mm (2.4 in.) in height, 100 mm (3.9 in.) in width, and 1000 mm (39.4 in.) in length. External drying was prevented by sealing the specimens immediately after casting using two layers of polystyrene sheets. External restraint between the specimen and the stainless steel rig was kept to a minimum by placing a soft, flexible, 2 mm (0.08 in.) thick foam rubber between the rig and the sealed specimen. The curing temperature was maintained at  $23 \pm 1^\circ C$  ( $73 \pm 2^\circ F$ ) by circulating water at a constant temperature of  $23^\circ C$  ( $73^\circ F$ ) through the double-walled chamber built into the sides and bottom of the rig. One end of the specimen was

fixed to the rig and the other end was free to move horizontally. The free end had a linear variable displacement transducer (LVDT) attached for measuring the autogenous deformation continuously and data were recorded every 10 minutes. Ten hours after mixing was the starting point for autogenous strain measurements on duplicate specimens. Average strain values are reported.

### Thermo-gravimetric analysis

The phase changes in hardening cement paste were investigated using thermo-gravimetric analysis (TGA). TGA measures the weight loss of a pulverized, hydrated cement paste sample that is subjected to heating from 25 to 1000°C at a heating rate of 10°C/min in a flowing argon (Ar) atmosphere. A typical TGA weight-versus-temperature curve and DTGA curve (first derivative of the weight loss curves versus temperature) is shown in Fig. 2.

The procedure for preparing TGA samples is as follows. First, the cement paste was cast into a mold and rotated on a roller until hardening to avoid segregation. The samples were then sealed and cured until the desired age. A slice of paste was subsequently taken and soaked in methanol to stop hydration and prevent carbonation. Methanol soaking was continued for at least 1 week prior to testing. The samples were then ground into a powder using a mortar and pestle, and were immediately used for thermal analyzer testing.

TGA was normally used to quantify the chemically bound water or nonevaporable water content  $w_m$ , which is the total water loss between approximately 105 and 1000°C (221 and 1832°F) less the weight loss contributed by the decomposition of carbonation products,  $w_{CO}$ , which occurs in the temperature range of approximately 600 to 800°C (1112 to 1472°F).<sup>14,15</sup> To some extent, various hydrate phases decompose (liberate their water) at different temperatures or over different temperature ranges. Although these ranges considerably overlap, some distinction can be made between calcium hydroxide (CH) and other hydrates, which include the primary product of hydration, calcium silicate hydrate (C-S-H). As demonstrated in Fig. 2, the presence of mass loss between 105 and 400°C (221 and 752°F) includes the loss of water associated with the amorphous and porous hydration products (PHPs), the majority of which is the C-S-H gel.<sup>16</sup> The weight loss computed over this temperature range will thus be referred to as  $PHP_{loss}$ . Calcium hydroxide is mostly crystalline and nonporous, and it decomposes between approximately 400 and 500°C (752 and 932°F). Therefore, the DTGA peak shown in Fig. 2 is more narrow and well-defined over this temperature range. The weight loss between 400 and 500°C (752 and 932°F) will be referred to as  $CH_{loss}$ . By knowing the water held in the various hydrates or hydrate groups, the development of these hydration products, which are of special interest, can be monitored and related to the physico-mechanical properties, including autogenous shrinkage and compressive strength.

## RESULTS AND DISCUSSION

### Autogenous shrinkage as result of self-desiccation due to cement hydration

Results in Fig. 3(a) show the measured autogenous shrinkage of neat OPC pastes at  $w/cm$  ranging from 0.35 to 0.45. As expected, the autogenous shrinkage increases with decreasing  $w/cm$ . Although the true mechanism behind autogenous shrinkage has been under debate, it is commonly thought that the reduction of pore humidity (self-

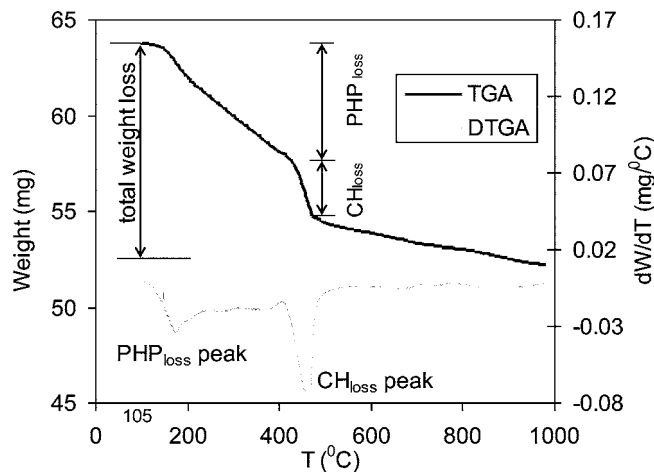


Fig. 2—TGA and DTGA curves for cement paste sample after 180 days of hydration.

desiccation) activates internal stresses (for example, capillary tension, disjoining pressure, surface tension), similar to drying shrinkage at the material level. To validate the hypothesis of self-desiccation as a major cause of autogenous shrinkage, the pore humidity reduction was simulated for the experimental paste material compositions. The pore RH is the ratio of the vapor pressure in the pore (which reflects the pore size and associated surface curvature due to confinement) to the saturated vapor pressure in an unconfined space. Pore humidity was predicted using HYMOSTRUC,<sup>3,4</sup> which is a microstructure-based model. This model can predict internal pore humidity reduction for different cement compositions and fineness and has been proved to be a reliable predictor of internal pore humidity for early-age hydrating cementitious materials.<sup>4</sup>

As illustrated in Fig. 3(b), pore humidity drops rapidly within the first few days with the greatest reduction of pore humidity observed for  $w/cm = 0.35$ , consistent with autogenous shrinkage observations. The lower the pore humidity, the less the amount of free capillary water held in cement paste. Thus, at low  $w/cm$ , the amount of anhydrous cement particles exposed to water and the space available for hydration products are reduced. It is well established that sealed hydration ceases when the internal pore RH reaches 70<sup>17</sup> to 75%.<sup>5,18</sup>

A unique correlation between autogenous shrinkage development and pore humidity reduction was obtained, which is approximately independent of  $w/cm$  (0.35 to 0.45), as shown in Fig. 4. The linear regression equation with an  $R^2$  value of 0.89 can be used for predicting autogenous shrinkage of a portland-cement paste,  $\epsilon_p$ , within the pore humidity range between 100 and 80%

$$\epsilon_p = \left[ 6150 \cdot \left( 1 - \frac{RH}{100} \right) \right] \times 10^{-6} \quad (1)$$

where  $RH$  is pore RH in percentage. A linear regression equation between shrinkage and pore humidity has been reported for concrete by Jonasson et al.<sup>19</sup>

### Unified concrete shrinkage model from paste measurement

Both autogenous and drying shrinkage are paste properties. The practicality of Eq. (1) can be enhanced if it

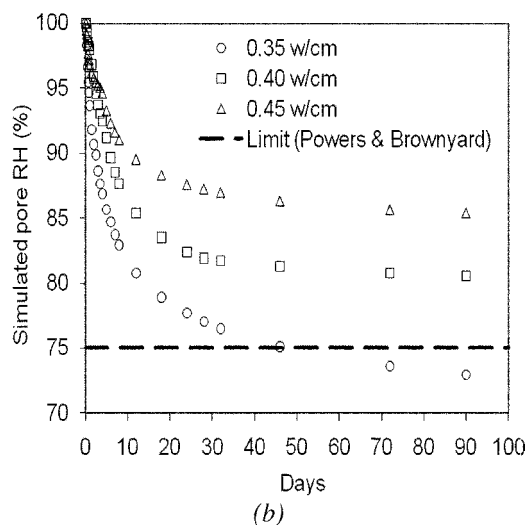
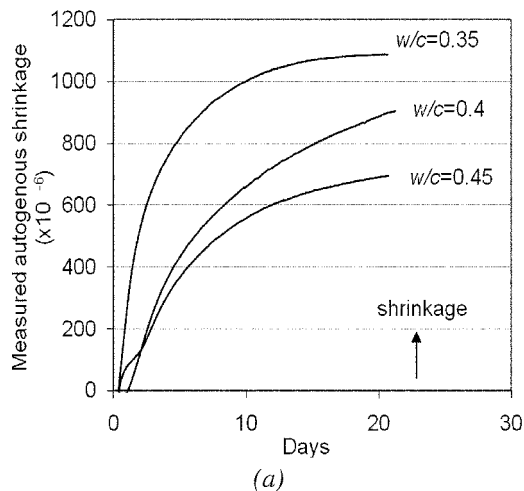


Fig. 3—Development of: (a) autogenous shrinkage; and (b) pore humidity of OPC paste at three w/cm of 0.35, 0.4, and 0.45.

can be applied to predict concrete autogenous shrinkage. This is tested further using the Pickett model<sup>20</sup>

$$\varepsilon_C = \varepsilon_P \cdot (1 - V_A)^n \quad (2)$$

where  $\varepsilon_C$  is shrinkage of concrete,  $\varepsilon_P$  is shrinkage of the paste,  $V_A$  is volume fraction of the aggregates, and  $n$  is a correlation parameter controlled by aggregate restraining effects, termed as shrinkage restraint factor in this study.

Experimental measurements were first made on concrete systems containing 40% aggregate by volume at w/cm of 0.35, 0.4, and 0.45. The measured concrete shrinkage results are plotted in Fig. 5 along with measured paste shrinkage results, showing that the addition of 40% aggregate by volume greatly reduces concrete autogenous shrinkage. The measured concrete autogenous shrinkage was then plotted versus paste autogenous shrinkage for all three w/cm. As shown in Fig. 6, regardless of different w/cm, all points fall approximately on one curve. The Pickett type expression provides an excellent fit, as shown by the solid line. An optimized  $n$  value of 1.68 was obtained for  $V_A = 40\%$  concrete, which is within the normal range of  $n$  values found for drying shrinkage, which typically vary between 1.2 and 1.9.<sup>20,21</sup>

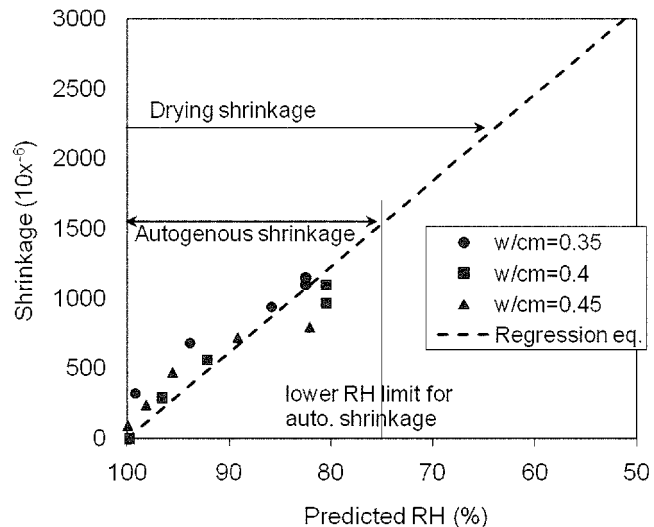


Fig. 4—Relationship of shrinkage and pore humidity of OPC paste at three w/cm of 0.35, 0.4, and 0.45.

It has been suggested that autogenous shrinkage is a special class of drying shrinkage.<sup>22</sup> Drying shrinkage spans a wider RH range and is typically measured at 50% RH, whereas autogenous shrinkage is limited to a more narrow RH range (not less than 75%). Therefore, it is acceptable to extend the linear curve of shrinkage versus RH obtained from an autogenous shrinkage result (Fig. 4, Eq. (1)) to the lower RH range to account for the drying shrinkage effect. Thus, the regression equations (Eq. (1) and (2)) developed for shrinkage predictions indicate that shrinkage at 75% RH is 0.54 of the shrinkage at 50% RH. This is consistent with shrinkage results of a 0.30 w/cm concrete where the autogenous to drying shrinkage ratio of 0.5 has been reported.<sup>23</sup>

The linearity in shrinkage-versus-RH relation (for example, Eq. (1)) for paste or concrete is reasonable from both capillary stress and surface-tension mechanism points of view. HYMOSTRUC simulations predict that internal pore stresses from the surface tension mechanism proportionally increase with the reduction in  $\ln(RH/100)$  between 100 and 50% RH. The same can be stated for the capillary stress mechanism as pore stresses are proportional to  $\ln(RH/100)$  in this humidity range. Thus, irrespective of whether capillary stress or surface-tension mechanism dominates, it is not unexpected that a linear regression equation (Eq. (1) as shown in Fig. 4) has been found for both autogenous and drying shrinkage in relation to RH.

The present findings suggest that an expression such as the one presented in Eq. (2) can be a unified model for shrinkage prediction in general. Model development based on autogenous shrinkage measurements has a major advantage over drying shrinkage because self-desiccation (that is, pore RH) is uniform, whereas pore RH is highly nonuniform in drying shrinkage tests on concrete, as water loss is diffusion-controlled. Thus, drying shrinkage measurement requires much longer testing times (1 year or more) to reach near-equilibrium conditions to develop a predictive model.

In the present study, the shrinkage restraint factor  $n$  was found to be 1.68. This value needs testing for each case and can be effectively obtained from autogenous shrinkage test results as shown herein for a given aggregate volume concentration. In general, a unified concrete shrinkage equation may look like

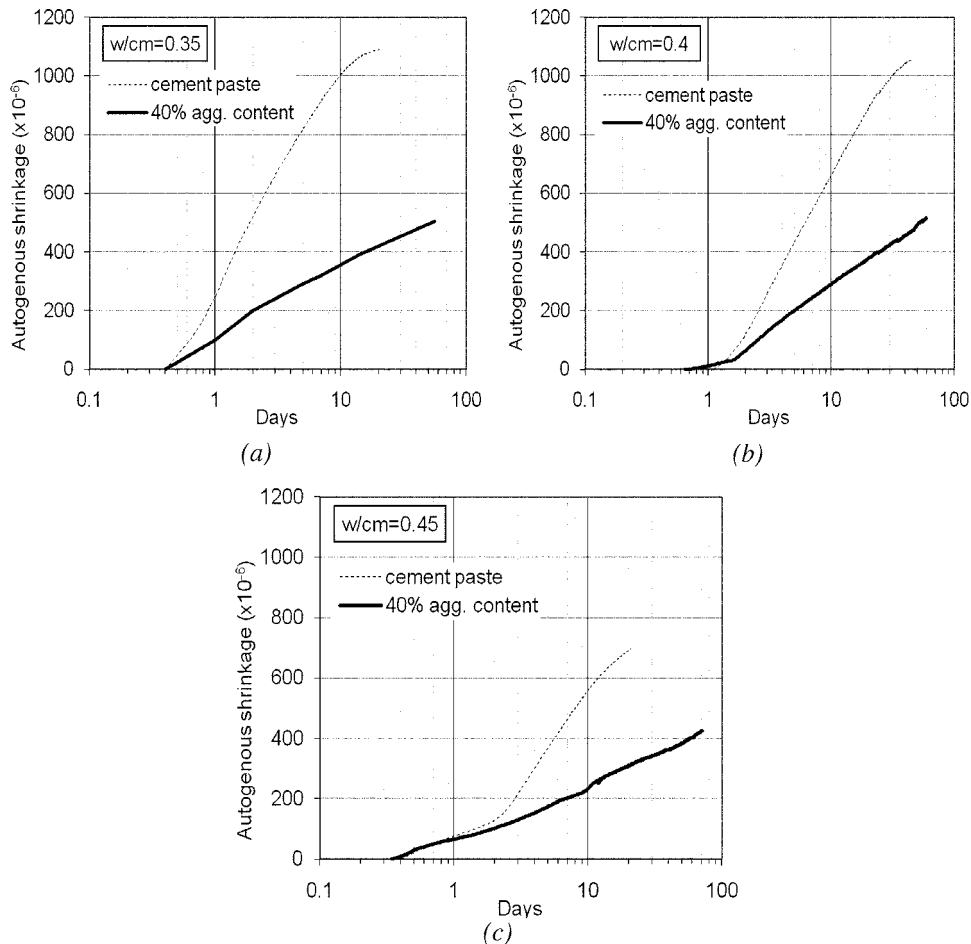


Fig. 5—Aggregate effect on autogenous shrinkage of concrete containing 40% aggregate by volume at: (a)  $w/cm = 0.35$ ; (b)  $w/cm = 0.4$ ; and (c)  $w/cm = 0.45$ .

$$\epsilon_C = \left[ 6150 \cdot \left( 1 - \frac{RH}{100} \right) \right] \cdot (1 - V_A)^n \times 10^{-6} \quad (3)$$

A further advantage of this expression is the ability to control ultimate shrinkage through aggregate volume adjustment (for example,  $V_A$  range of 60 to 70%) and early-age (0 to 7 days) autogenous shrinkage development through  $w/cm$  control (0.35 to 0.45), as seen from Fig. 3.

Predicted results of concrete shrinkage are plotted in Fig. 6 for three aggregate volume percentages ( $V_A = 60, 65,$  and  $70\%$ ) versus paste shrinkage. In the case of high paste shrinkage of 1000 to  $1200 \times 10^{-6}$ , concrete shrinkage can be reduced to less than 200 to  $300 \times 10^{-6}$  through mixture proportioning adjustments (that is, increasing aggregate content to approximately 65 and 70%, as shown in Fig. 6). Thus, aggregate adjustment is an effective way to control autogenous shrinkage development and ultimate concrete shrinkage.

### GGBFS effect on autogenous shrinkage and hydration characteristics

The measured autogenous shrinkage of cement paste containing GGBFS ranging from 0 to 50% of the total cementitious materials by weight is shown in Fig. 7 for  $w/cm = 0.35$  and 0.45. A direct interpretation from Fig. 7 suggests that GGBFS reduces early-age autogenous shrinkage while the longer-term shrinkage is increased. The reduction in

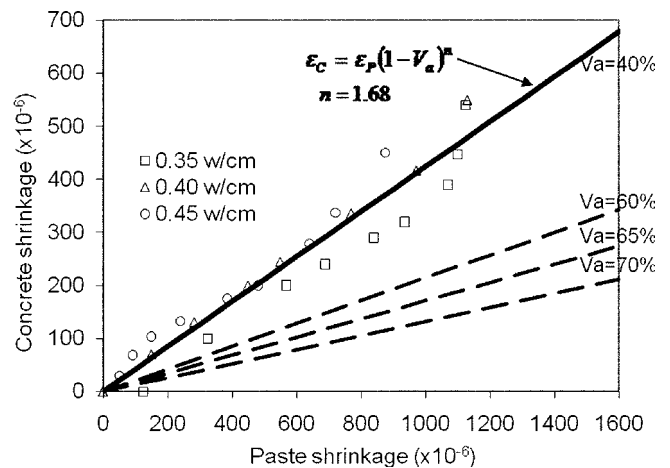


Fig. 6—Relationship of concrete and paste autogenous shrinkage at three  $w/cm$  of 0.35, 0.4, and 0.45.

early-age shrinkage is because GGBFS pozzolanic reaction is initially slower than the hydration of cement. As long as GGBFS behaves like a filler (that is, prior to the onset of pozzolanic reactivity), an increase in GGBFS content by total cementitious material is analogous to increasing the effective  $w/cm$ , thus reducing early-age autogenous shrinkage. With the increase of degree of hydration, a high

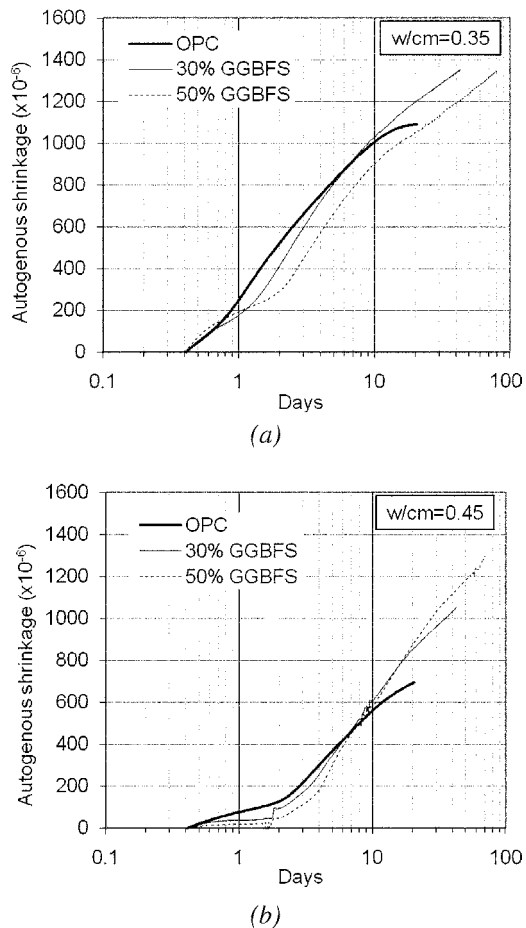


Fig. 7—Development of autogenous shrinkage of cement paste with GGBFS content ranging from 0% and 30 to 50% at: (a)  $w/cm = 0.35$ ; and (b)  $w/cm = 0.45$ .

internal RH condition may exist in a higher  $w/cm$  paste (for example, 0.45), whereas the internal RH in a 0.35  $w/cm$  system is approaching the lower limit (approximately 75% RH). Therefore, it is hypothesized that long-term pozzolanic reactions can proceed in a 0.45  $w/cm$  paste, pushing the internal RH lower. This, in turn, increases long-term autogenous shrinkage in a higher  $w/cm$  system containing GGBFS until the internal RH approaches 75%.

To better understand the mechanism of why GGBFS causes continuous growth of autogenous shrinkage at later ages, TGA was conducted as a complementary method to the traditional experimental measurement of autogenous shrinkage. It was found in this study that the increasing content of PHPs is closely related to the continuous growth of autogenous shrinkage in a GGBFS blended system. As shown in Fig. 8(a) and (c) for both  $w/cm = 0.35$  and 0.45 pastes with 30 and 50% GGBFS contents, curves exhibit a sharp increase in  $PHP_{loss}$  after approximately 7 days of hydration, and a somewhat sustained higher slope thereafter and a greater amount of  $PHP_{loss}$  at later ages. This is consistent with the autogenous shrinkage growth behavior shown in Fig. 7 that, after approximately 7 days, greater autogenous shrinkage was observed in GGBFS blended system. The PHPs such as C-S-H have substantial surface area, greater than  $200 \text{ m}^2/\text{g}$ , which is at least an order of magnitude greater than any other components in hardened portland-cement paste.<sup>24</sup> This magnifies the effect of the capillary or surface-tension stresses, which both can be the driving

forces for the development of autogenous shrinkage. Although an increase in PHPs will result in a decrease in capillary porosity, it appears that the increase in net surface area outweighs the reduction in capillary pore volume in terms of their influence on autogenous shrinkage development, while for another major hydration product, CH, it is usually thought that crystalline CH works as a restraint upon shrinkage of porous phase in paste, and thus the consumption of CH due to pozzolanic reactions results in greater shrinkage.<sup>7,10</sup> From Fig. 8(b) and (d), it is seen that the CH content is lower in GGBFS systems due to the dilution of OPC by GGBFS. A reduction of CH content due to pozzolanic reaction, however, was not observed in this study, as illustrated in Fig. 9; this is detailed in the following.

Because the solid substances, along with water, in a hydrating paste play a key role in shrinkage behavior, it is of significance to evaluate GGBFS contributions to the two major hydration products. Considering the complexity of SCM reactions, the contribution of GGBFS to PHP is simply evaluated as  $PHP_{con} = PHP_{mea} - f_{OPC} \cdot PHP_{OPC}$ , where  $PHP_{con}$  is GGBFS contribution to PHP,  $PHP_{mea}$  is measured PHP of a blended system,  $f_{OPC}$  is OPC content in the blended system by mass,  $PHP_{OPC}$  is measured PHP of a pure OPC system, and  $f_{OPC} \cdot PHP_{OPC}$  represents PHP in a blended system assuming no pozzolanic reaction and treating the GGBFS only as an unreactive filler. Thus, the actually measured PHP minus PHP, calculated assuming no pozzolanic reaction, is treated as GGBFS contribution to PHP in a blended system. GGBFS contribution to CH content was calculated the same way. The results are shown in Fig. 9, demonstrating that GGBFS pozzolanic reaction has significant influence on the production of PHP, and 50% GGBFS content shows greater contribution than 30% GGBFS. The time when GGBFS contribution to PHP is pronounced starts at approximately 7 days. Pozzolanic reaction, however, has minor effect on CH content, suggesting that GGBFS pozzolanic reaction does not cause significant amounts of CH reduction due to the fact that GGBFS itself has latent hydraulic properties and can react with water and produce CH. Therefore, the general assumption that pozzolanic reactions result in increasing shrinkage due to the consumption of CH (working as a shrinkage restraint) is most likely not the main reason why long-term shrinkage is increased in a GGBFS system.

According to Eq. (2), the autogenous shrinkage of concrete containing GGBFS can be predicted from the paste shrinkage measurement as well. Predictions shown in Fig. 10 for the 90-day autogenous shrinkage of a GGBFS blended system suggest a reduction from approximately  $1400 \times 10^{-6}$  of the paste (refer to Fig. 7) to less than  $200 \times 10^{-6}$  of the concrete containing 70% aggregate by volume. Thus, the increase in long-term paste shrinkage from pozzolanic effect can be compensated for by using an appropriate amount of aggregate in the concrete mixture design. Overall, the incorporation of GGBFS is expected to improve early-age cracking resistance due to the filler effect that increases the effective  $w/cm$ , thus reducing early-age autogenous shrinkage while ensuring the positive long-term durability enhancements associated with pozzolanic reactions. The tendency for increased long-term paste shrinkage due to pozzolanic effects can be effectively compensated for in concrete through aggregate volume adjustment.

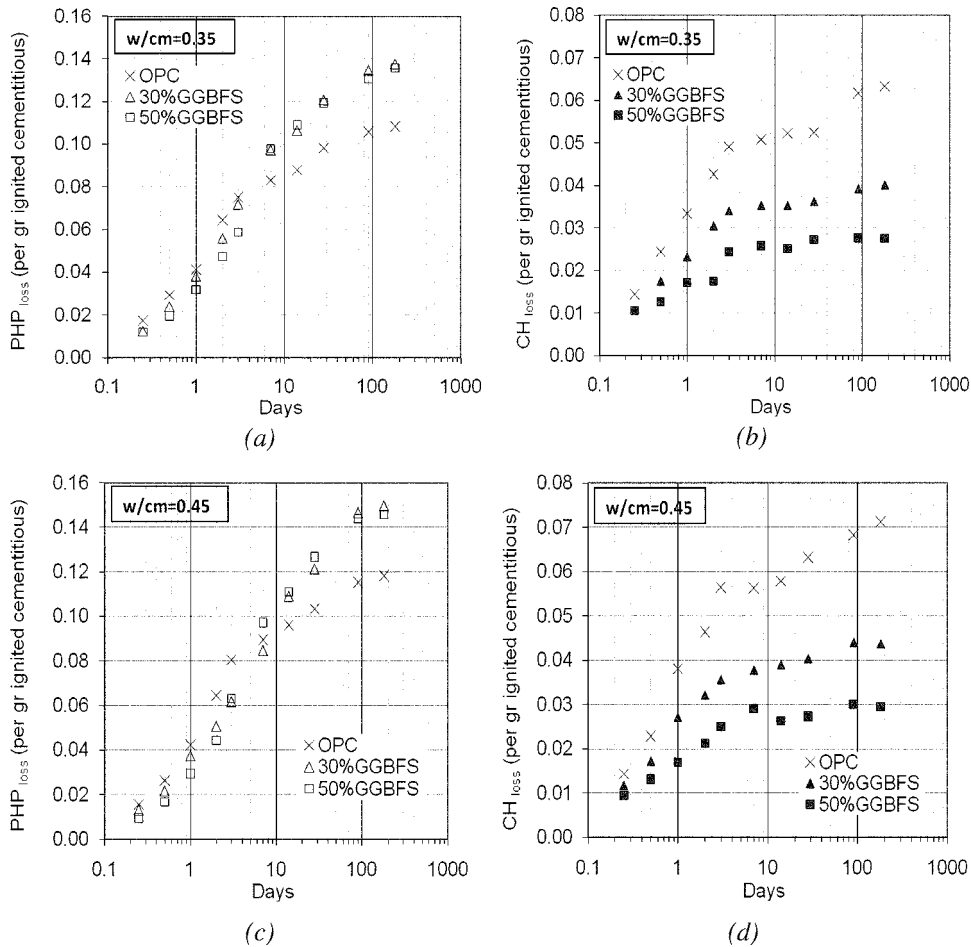


Fig. 8—Development of PHP and CH in cement paste with GGBFS content ranging from 0% and 30 to 50% at  $w/cm = 0.35$  and  $0.45$ .

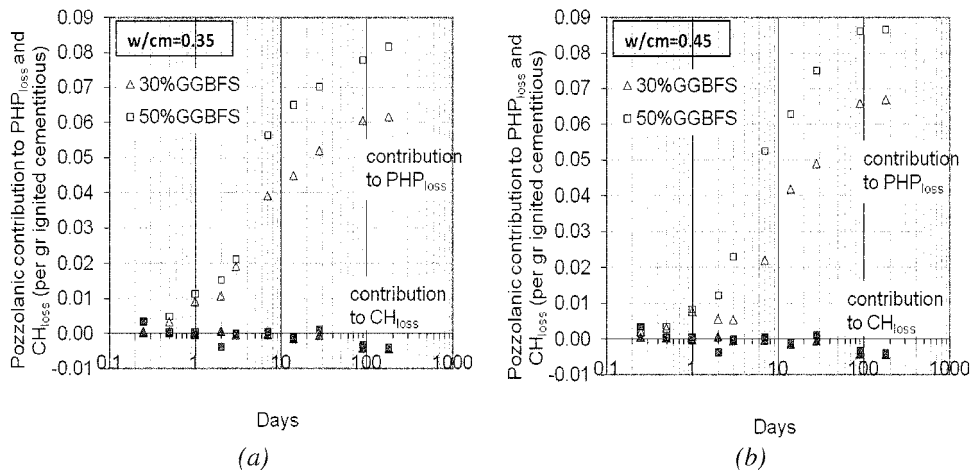


Fig. 9—Contribution of pozzolanic reaction to development of PHP and CH for  $w/cm = 0.35$  and  $0.45$ .

### CONCLUSIONS

The results of this experimental investigation provide a phenomenological basis for better understanding the mechanism of autogenous shrinkage and development of environmentally friendly and sustainable concrete. The major findings of this study are:

1. The overall driving force for autogenous shrinkage is self-desiccation (reduction in pore RH) within the PHPs from sealed hydration. The self-desiccation effect is  $w/cm$

and time-dependent and explains why autogenous shrinkage is pronounced in low- $w/cm$  (less than 0.40) systems. The data presented in this study show that autogenous shrinkage development in hydrating paste is uniquely related to the reduction in pore humidity, and approximately independent of  $w/cm$  (0.35 to 0.45). Self-desiccation, however, limits autogenous shrinkage to the pore humidity range between 100% RH and 70 to 75% RH when hydration ceases.

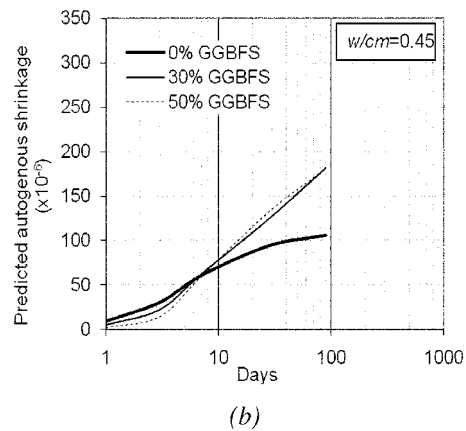
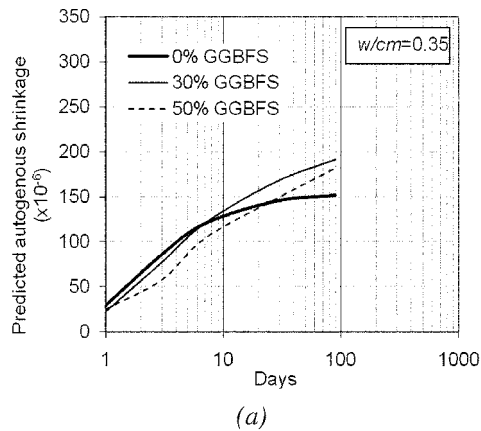


Fig. 10—Predicted autogenous shrinkage of concrete containing 70% aggregate by volume and GGBFS ranging from 0 to 50% at: (a)  $w/cm = 0.35$ ; and (b)  $w/cm = 0.45$ .

2. The effect of aggregate on autogenous shrinkage reduction was found to follow a Pickett-type model that was developed for drying shrinkage prediction. The results presented herein suggest that autogenous shrinkage and drying shrinkage are one and the same phenomenon, as they both occur due to reduction in pore RH. A unified shrinkage model for autogenous and drying shrinkage is proposed based on expected RH of pore-drying, aggregate volume fraction, and restraint factor for concrete. The restraint factor is determined from autogenous shrinkage results as well.

3. GGBFS reduces early-age (0- to 7-day) shrinkage, as pozzolanic reactions are initially slower than cement hydration reactions, whereas long-term autogenous shrinkage is larger than that of the pure paste with the same  $w/cm$ . This effect is especially pronounced in higher  $w/cm$  (0.45) systems, whereas long-term autogenous shrinkage can reach similar values as for low- $w/cm$  (0.35) pastes for the same GGBFS content. From a hydration products point of view, this behavior is most likely related to the increasing PHP content other than the consumption of crystalline CH. This increase in longer-term shrinkage in GGBFS concrete systems can be effectively offset by slightly increasing the aggregate volume concentration.

#### ACKNOWLEDGMENTS

This material is based on work supported by the National Science Foundation under Grant No. 0510854. Any opinions, findings, and conclusions or recommendations expressed in this material are those of the author(s) and do not necessarily reflect the views of the National Science Foundation. The authors wish to thank E. A. B. Koenders for his assistance with the modifications to the HYMOSTRUC software.

#### REFERENCES

1. Copeland, L. E., and Bragg, R. H., "Self-Desiccation in Portland Cement Pastes," *Research Department Bulletin RX052*, Portland Cement Association, Skokie, IL, 1955, 112 pp.
2. ACI Committee 231, "Report on Early-Age Cracking: Causes, Measurement, and Mitigation (ACI 231R-10)," American Concrete Institute, Farmington Hills, MI, 2010, pp. 1-46.
3. Van Breugel, K., "Simulation of Hydration and Formation of Structure in Hardening Cement-Based Materials," PhD thesis, Delft University of Technology, Delft, the Netherlands, 1991, 295 pp.
4. Koenders, E. A. B., "Simulation of Volume Changes in Hardening Cement-Based Materials," PhD thesis, Delft University of Technology, Delft, the Netherlands, 1997, 171 pp.
5. Powers, T. C., and Brownyard, T. L., "Studies of the Physical Properties of Hardened Portland Cement Paste," *ACI JOURNAL*, *Proceedings* V. 43, No. 9, 1947, p. 971.
6. Powers, T. C., "A Discussion of Cement Hydration in Relation to the Curing of Concrete," *Proceedings*, Highway Research Board, V. 27, 1947, p. 178.

7. Jensen, O. M., and Hansen, P. F., "Autogenous Deformation and Change of the Relative Humidity in Silica Fume-Modified Cement Paste," *ACI Materials Journal*, V. 93, No. 6, Nov.-Dec. 1996, pp. 1238-1249.
8. Bentz, D. P.; Jensen, O. M.; Hansen, K. K.; Oleson, J. F.; Stang, H.; and Haecker, C. J., "Influence of Cement Particle Size Distribution on Early Age Autogenous Strains and Stresses in Cement-Based Materials," *Journal of the American Ceramic Society*, V. 84, No. 1, 2001, pp. 129-135.
9. Hanehara, S.; Hirao, H.; and Uchikawa, H., "Relationship between Autogenous Shrinkage and the Microstructure and Humidity Changes at Inner Part of Hardened Cement Pastes at Early Ages," *Proceedings of the International Workshop Autoshrink '98*, E.-I. Tazawa, ed., Hiroshima, Japan, E&FN Spon, London, UK, 1999, pp. 89-100.
10. Lura, P., "Autogenous Deformation and Internal Curing of Concrete," Delft University of Technology, Delft, the Netherlands, 2003, 180 pp.
11. Lee, K. M.; Lee, H. K.; Lee, S. H.; and Kim, G. Y., "Autogenous Shrinkage of Concrete Containing Granulated Blast-Furnace Slag," *Cement and Concrete Research*, V. 36, 2006, pp. 1279-1285.
12. Mindess, S.; Young, J. F.; and Darwin, D., *Concrete*, second edition, Prentice Hall, Englewood Cliffs, NJ, 2003, 644 pp.
13. Schleibinger, "Manual of Schleibinger Shrinkage-Cone and Shrinkage-Drain, Bending-Drain and Thin-Layer-Shrinkage-System," 2007, 37 pp.
14. Mackenzie, R., *Differential Thermal Analysis. Volume 1—Fundamental Aspects*, Academic Press, 1970, p. 775.
15. Pane, I., and Hansen, W., "Investigation of Blended Cement Hydration by Isothermal Calorimetry and Thermal Analysis," *Cement and Concrete Research*, V. 35, 2005, pp. 1155-1164.
16. Melo Neto, A. A.; Cincotto, M. A.; and Repette, W., "Drying and Autogenous Shrinkage of Pastes and Mortars with Activated Slag Cement," *Cement and Concrete Research*, V. 38, 2008, pp. 565-574.
17. Nilsson, L. O., and Mjornell, K., "A Macro-Model for Self-Desiccation in High Performance Concrete," *Report TVBM-3126*, Proceedings of the Fourth International Research Seminar on "Self-Desiccation and its Importance in Concrete Technology," Gaithersburg, MD, June 2005, pp. 49-66.
18. Jensen, O. M., "Thermodynamic Limitation of Self-Desiccation," *Cement and Concrete Research*, V. 25, No. 1, 1995, pp. 157-164.
19. Jonasson, J.-E.; Groth, P.; and Hedlund, H., "Modeling of Temperature and Moisture Field in Concrete to Study Early Age Movements as a Basis for Stress Analysis," *RILEM Proceedings 25 of Thermal Cracking in Concrete at Early Ages*, 1998, pp. 45-54.
20. Pickett, G., "Effect of Aggregate on Shrinkage of Concrete and Hypothesis Concerning Shrinkage," *ACI JOURNAL*, *Proceedings* V. 52, No. 1, Jan. 1956, pp. 581-590.
21. L'Hermite, R. G., "Volume Changes of Concrete," *Fourth International Symposium on the Chemistry of Cement*, Washington, DC, 1960, pp. 659-702.
22. Grasley, Z. C., "Measuring and Modeling the Time-Dependent Response of Cementitious Materials to Internal Stresses," PhD thesis, University of Illinois at Urbana-Champaign, Urbana, IL, 2006, 216 pp.
23. Kosmatka, S. H.; Kerkhoff, H.; and Panarese, W. C., *Design and Control of Concrete Mixtures*, 14th edition, EB001, Portland Cement Association, Skokie, IL, 2002, 358 pp.
24. Roy, D. M., and Idorn, G. M., "Hydration, Structure and Properties of Blast Furnace Slag Cements, Mortars, and Concrete," *ACI Materials Journal*, V. 79, No. 6, June 1982, pp. 444-457.